Monte-Carlo simulations of cosmic-ray and internal radiation effects on ISOCAM on board ISO

Arnaud Claret (arnaud.claret@cea.fr) and Hervé Dzitko
CEA-Saclay, Service d'Astrophysique, 91191 Gif-sur-Yvette Cedex, France

Abstract. One of the main limitations to the sensitivity of the infrared camera ISOCAM on-board the Infrared Space Observatory (ISO) comes from responsivity variations and glitches caused by the impacts of charged particles in photo-detectors. Glitch rate measurements, glitch properties and removal methods have already been addressed during the first ISO detector workshop (Madrid, 1998) and published in a special issue of Experimental Astronomy. It appeared that glitch rate and most of glitch properties could be reproduced by Monte-Carlo simulations. This is very interesting in order to predict before launch the effect of charged particles in photo-detectors operated in space. This paper presents results of Monte-Carlo simulations of radiation effects on ISOCAM detectors. Glitch rates, spatial and energetic properties of glitches have been computed and are compared with measured values.

Keywords: Monte-Carlo methods, radiation effects, CCD, ISO spacecraft

1. Introduction

During the first Infrared Space Observatory (ISO) detector workshop (Madrid, 1998), a number of detailed technical reports of the performance of ISO detectors were presented, along with more general discussions on glitch effects (Claret et al., 2000), transient effects and future detector strategies, particularly in view of the upcoming HERSCHEL (previously named FIRST) and NGST (Next Generation Space Telescope) missions. The so-called glitch phenomenon is the result of an energy deposit from charged particles in detectors operating in space. This phenomenon requires detailed knowledge of the cosmic ray environment, trapped electron and proton fluxes, and other space environmental parameters. An international glitch working group has been created in order to provide information on the radiation environment of the ISO orbit during the mission (1995-1998). Analysis of glitch effects in the four ISO (Kessler et al., 1996) instruments (ISOCAM camera, ISOPHOT photometer, ISOLWS long wave spectrometer, and ISOSWS short wave spectrometer) is indeed of great interest to prepare future space experiments, such as HERSCHEL or NGST.

After more than 28 months of successful operations, the first measurement of glitch effects in ISOCAM data was presented in Claret et al. (2000). The predicted glitch rate was re-evaluated after the launch

and compared to in-flight measurements. The glitch removal methods were also addressed in this paper. A more general discussion of the glitch phenomenon was presented in Claret et al. (1999), giving an interpretation of spatial and temporal profiles of glitches. The study of temporal and spatial properties of glitches has led to a classification into 3 distinct families. These families are related to the Linear energy Transfer (LET) of charged particles interacting with the detectors. Analytical prediction of glitch rate, as well as theoretical track length of glitches, can be found in (Dzitko et al., 2000). However analytical predictions are generally limited to the assessment of average values rather than distributions of interesting parameters (such as deposited energy, particle track length, glitch rate, ...). Monte-Carlo simulations are thus helpful to provide these distributions, in order to assess precisely the induced noise level on detectors. This paper is focused on Monte-Carlo simulations of radiation effects on ISOCAM. This simulation tool could then be calibrated using in-flight data. It is possible to use this tool in order to simulate radiation effects for future space experiments.

After a brief description of the ISOCAM radiation environment (Section 2), predictions of radiation effects on ISOCAM are compared to in-flight measurements (Section 3). The radiation environment and the geometrical model of Monte-Carlo simulations are described in Section 4. Several kinds of incident particles were considered : galactic particles (protons and alphas) and also internal particles (alphas) generated by the coating of lenses. Results are compiled in Section 5. These results are discussed in Section 6, while conclusions and perspectives are presented in Section 7.

2. ISOCAM Radiation Environment

2.1. ISOCAM Camera

The ISOCAM camera was operated at very low temperature on board ISO from November 1995 until April 1998. The temperature of the telescope focal plane was 2.4 K thanks to passive helium cooling. All details about the ISOCAM camera can be found in (Cesarsky et al., 1996). We present here only the main characteristics relevant for Monte-Carlo simulations. The infrared camera ISOCAM was designed to operate in the 2.5-17 μm range with two detectors of 32×32 pixels (see Fig. 1):

– A long wave (LW) detector using a SiGa substrate with a Direct Readout Output circuit, for 4-17 μm wavelengths. LW detector had a 100 μm pitch and a thickness of 500 μm.

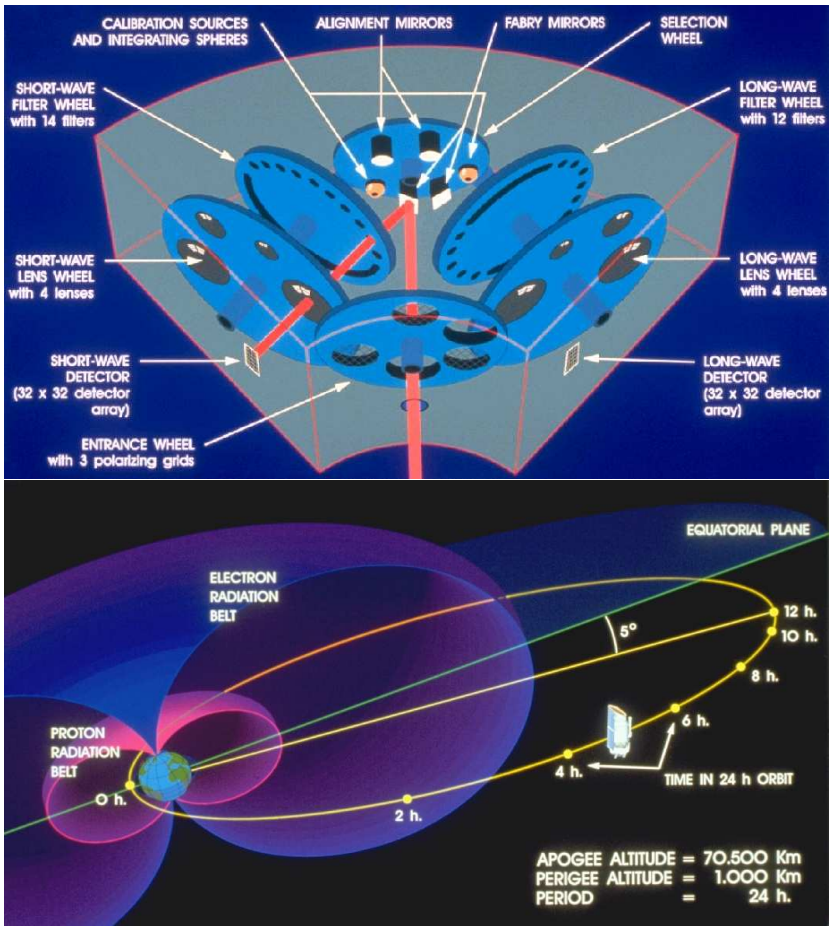

Figure 1. Cut-away of the ISOCAM camera on board of the ISO spacecraft (upper panel). Main parameters of the ISO orbit (lower panel).

– A short wave (SW) detector using a InSb substrate and a Charge Injection Device readout method, for 2.5-5 μm wavelengths.

Active zone of SW pixels was very thin (less than 10 μm), so that it had a low susceptibility to radiation effects. The LW detector was much thicker (500 μm). This led to a much higher susceptibility to radiation effects (see Section 3.1).

2.2. ISOCAM Orbit And Space Environment

The ISO telescope was operated in a highly elliptical 24-hour orbit with a perigee at 1,000 km and an apogee at 70,500 km (see Fig. 1). The lowest part of the orbit lied inside the Earth's van Allen belts. Inside the belts, the majority of ISO's detectors were scientifically

unusable due to effects caused by proton and electron impacts. Outside the radiation belts (roughly 16 hours), the spacecraft was directly exposed to galactic cosmic rays (GCRs). GCRs are composed of 87% protons, 12% alphas, and 1% heavier nuclei. The differential spectrum of GCRs is roughly peaked at 500 MeV/n. Occasional solar particle events produced additional protons and heavier nuclei.

3. Radiation Effects on ISOCAM

3.1. Predicted Length Of Particle Tracks

The particle track length may be easily found only by geometrical considerations. Let Φ be the particle flux (in cm^{-2} s^{-1} sr^{-1}). The incoming flux (in s^{-1}) passing through the surface unit dS is given by (Sullivan, 1971):

$$\phi = \Phi \int_0^{\frac{\pi}{2}} 2\pi sin\theta dS\ cos\theta d\theta = \pi \Phi dS$$

If the detector shape is approximated by a rectangle parallelepiped, the incoming flux through all the faces is merely $\phi_{detector} = \pi\Phi \times 2(AB + BC + AC)$, where A, B and C are the dimensions of the detector. Similarly, the total flux traversing the set of N pixels of the detector is $\phi_{all\ pixels} = N \times [\pi\Phi \times 2(ab + bc + ac)]$, where a, b and c are the pixel dimensions. Assuming that the particles follow straight lines in the detector, the mean number $< n >$ of pixels per track is given by:

$$< n > \sim \frac{\phi_{all\ pixels}}{\phi_{detector}} = \frac{N \times (ab + bc + ac)}{(AB + BC + AC)}$$

Taking the number of pixels (N=1024), the pixel dimensions (a=b=0.01 cm and c= 0.05 cm) and the two detector dimensions (A=B=0.32 cm and C=0.05 cm for LW, A=B=0.32 cm and C=0.0005 cm for SW), the previous equation gives:

- 8.4 pixels per track for LW glitches,
- 0.8 pixels per track for SW glitches,

showing the lower sensitivity to particle impacts of the SW detector. Thus, only LW glitches will be addressed in this paper.

3.2. Predicted Glitch Rate

Our assessment of direct impacts is based on measurements by the KET (Kinetic Electron Telescope) on board of the Ulysses spacecraft (Oct-1997 and Feb-1998, when it was close to the ecliptic plane). The fluxes of protons and alphas (B. Heber and P. Ferrando, private communication) were taken from Paizis et al. (2001) and were divided by the geometrical factor found in Simpson et al. (1992). Another contribution comes from primary particles passing through the surrounding materials, producing additional events either by nuclear reactions or δ-ray emissions. In addition to these external particles, the anti-reflection coating of lenses contains traces of ^{232}Th, which generates a flux of low energy alpha particles. The flux of alpha particles depends on the solid angle of the lens viewed from the array, which depends of the lens used. The ^{232}Th contribution was maximum for the 12 arcsec/pixel lens. Fortunately, this lens was not often used due to its stronger distortion of the field of view. Note that there are two significant differences between alpha particles from GCRs and alpha particles from the lens coating. First, alphas from GCRs have enough energy to traverse the detector, whereas alpha particles from ^{232}Th are stopped in less than 20μm. Secondly, alphas from GCRs have an isotropic directional distribution whereas alpha particles from ^{232}Th hit the detector with a normal incidence. The latest estimation of glitch rate is given as a function of the pixel field of view together with an estimation of the errors on each contribution (see Table I).

Table I. Predicted glitch rate for LW detector (s^{-1}). The contribution of alphas produced by ^{232}Th is given as a function of the lens because it depends on the solid angle of the lens viewed from the array.

Origin of particles	**Contribution**				**Error**
Primary GCRs	0.36				∼10%
Secondary particles and δ-rays	0.29				factor 2
Lens (arcsec/pixel)	1.5	3	6	12	
Alphas produced by ^{232}Th	0.002	0.02	0.16	0.35	<10%
TOTAL	**0.65**	**0.67**	**0.81**	**1.0**	

Neither the electro-magnetic showers, nor the secondary particles from the body of spacecraft have been taken into account here. These last contributions are more difficult to derive and require Monte-Carlo simulations. The reader is referred to (Dzitko et al., 2000) for details

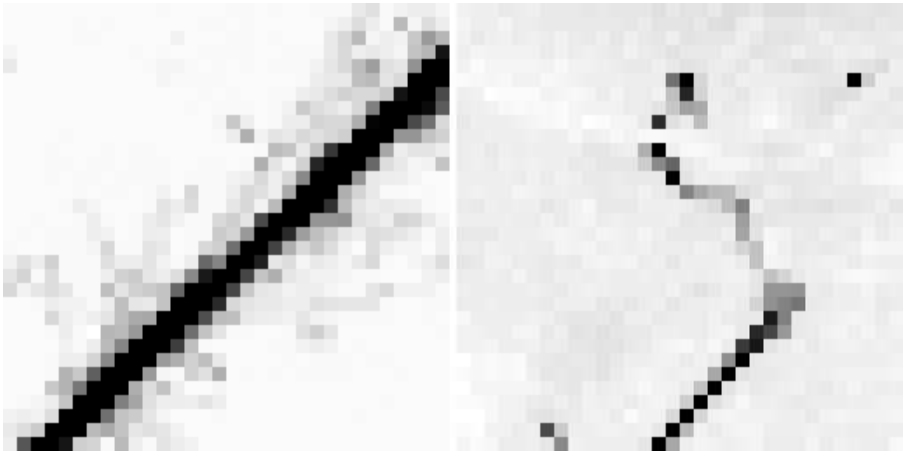

Figure 2. On the left image, the track is interpreted as high-energy heavy ion passing through the detector. δ-rays are clearly visible along the track. On the right image, a particle has stopped inside the detector. The incoming particle has collided a nucleus of the detector and the faint track might be the result of this recoil nucleus.

about the computation of these contributions. The error on the direct contribution (primary GCRs) is based on KET measurements and is assessed to be around 10%. The contribution of secondary particles and δ-rays has been taken equal to 80% of direct contribution. The error on this contribution is assessed to be a factor 2. Since the contribution of alpha particles produced by ^{232}Th was measured in the laboratory before the launch, the error on this contribution is assessed to be better than 10%.

3.3. In-flight Measurements

Some key numbers about ISOCAM glitches, as deduced from in-flight measurements, are:

- average glitch rate = 1 glitch/s,
- average number of hit pixels = 8 pixels/glitch.

These numbers are mean values and correspond to what should be observed during a standard ISOCAM observation (e.g. with 6 arcsec/pixel lens, and not during solar activity). See Claret et al. (1999) for more

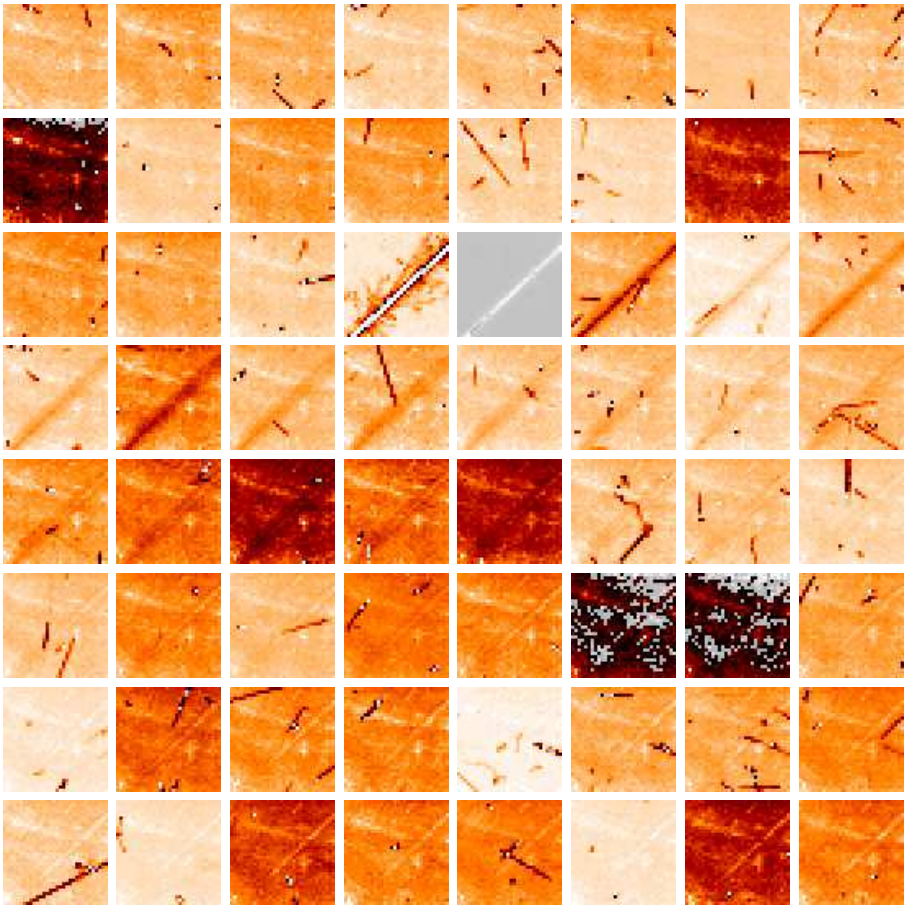

Figure 3. Set of successive images of the ISOCAM LW detector. The sequence of images goes from left to right and from top to bottom. Each image represents an integration time of 5.04 s. In order to improve the signal to noise ratio for astrophysical source detection, these individual images must be co-added but glitches have to be removed from images first. Glitch removal methods (Claret et al., 1999) were developed for that purpose. They were also used in order to measure the actual glitch rate during spacecraft operations. If the integration time of individual images is too long with respect to the rate of incoming particles, then images are too much polluted by glitch effects and cannot be corrected anymore. Images are then useless for science. This is the reason why the glitch rate must be evaluated before the launch, especially in order to choose the set of usable integration times for images. Occasionnaly, the flux of incoming particles can increase strongly (ie during solar flares) and images cannot be used for science. Generally, instruments must be shut down during several hours in case of solar activity. When the detector is traversed by an ion, the track can be visible during more than a minute.

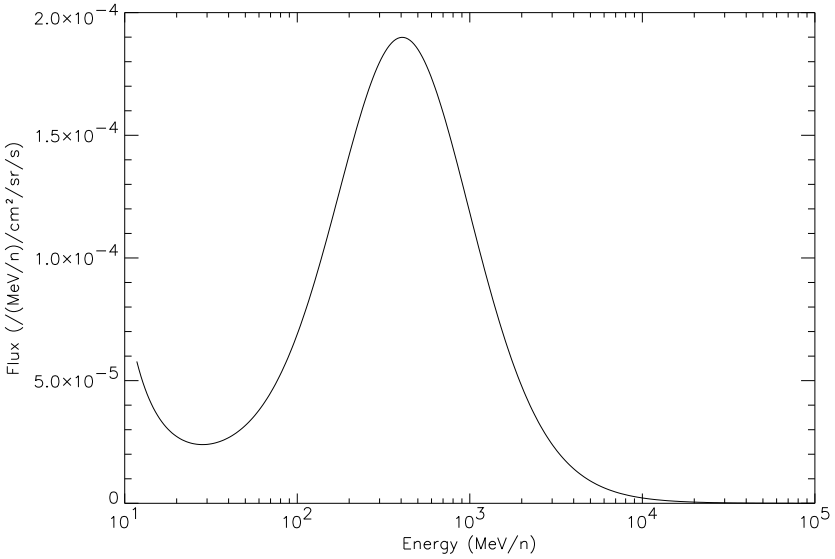

Figure 4. Galactic spectrum for protons. This spectrum was derived from Spacerad 4 (M=1 solar minimum) and the incoming flux was normalized with KET spacecraft data (see text).

details. More generally, glitch impacts represent a $\sim$1% sensitivity loss per second of integration. Actually, the sensitivity loss can be significatively higher due to glitch tails. It takes indeed a longer period of time for the detector to recover from it when the deposited energy is higher. The strongest glitches are induced by heavy ions (see Fig. 2). Since the LET of ion is high, several minutes are necessary for the detector to recover from it. For example, the remaining particle track is clearly visible on at least 20 images of 5 sec each on after the passage of a heavy ion (see Fig. 3).

4. Monte-Carlo Simulations

4.1. Radiation Environment

In this paper, we present simulations of particle effects from GCRs (protons and alphas) and also internal particles (alpha particles produced by traces of ^{232}Th contained in the anti-reflecting coating of lenses).

Spectra of galactic protons and alphas were computed by Spacerad 4 (Letaw, 1990-97) and normalized with measurements of protons made by KET when it was close to the ecliptic plane. But since the spacecraft body is equivalent to 2.5 cm of aluminum, only particles with

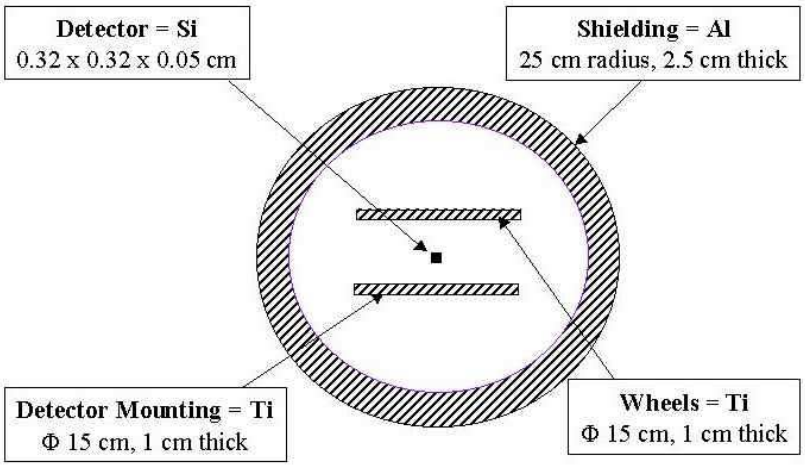

Figure 5. Simple geometrical model representing the detector and its surroundings.

energy greater than 80 MeV/n can traverse this shield. The integral spectra above this energy was compared to the KET spectra and the normalization factors deduced. The proton and alpha spectra produced by Spacerad 4 were then multiplied by the normalization factors. For information, these normalization factors were smaller than 1.2 for the integral spectra. Corresponding fluxes are 0.39 cm^{-2} sr^{-1} s^{-1} and 0.032 cm^{-2} sr^{-1} s^{-1} respectively for protons and alpha particles. This leads to the total flux for galactic cosmic rays of $\Phi_{GCRs} = 0.422$ cm^{-2} sr^{-1} s^{-1} and to the total number of direct impacts from primary GCRs (see Section 3.2 for details):

$$\begin{aligned} \phi_{Direct\ Impacts} &= \pi\ \Phi_{GCRs} \times 2(AB + BC + AC) \\ &= 0.844 \times \Phi_{GCRs} \\ &\sim 0.36\ s^{-1} \end{aligned}$$

For illustration purpose, the proton spectrum is displayed on Fig. 4. Alpha particles coming from radioactive coating of lenses have an energy of 4 MeV. Since they have to escape from the lens coating, their spectrum is not strictly mono-energetic when arriving on the detector. But it did not appear necessary to consider a attenuated spectrum for these alpha particles (see Section 5.3.).

4.2. Geometrical Model

In order to simplify the interpretation, the detector has been modeled as shown on Fig. 5. A simple geometry was used for modeling the lens and filter wheels, the detector mounting, and the spacecraft shielding. The

region of charge collection (ie the detector) was modeled as a rectangle parallelepiped. It was divided in 32×32 elementary volumes in order to simulate the pixels of the detector.

4.3. Monte-Carlo Runs

The GEANT Monte-Carlo code (version 3.1) was used to simulate the particle transport (CERN, 2000) of primary particle fluxes which were computed by Spacerad 4. Energy loss by ionisation, δ-ray generation, hadron interactions and multiple scattering have been simulated. GEANT calculates the energy loss following the particle through all interactions in true Monte-Carlo form.

Main parameters for the simulations of GCRs are given below:

- 13 energy bins between 100 MeV/n and 6 GeV/n for protons and alphas of isotropic incident direction with respect to the detector,
- 10 runs for each energy bin in order to reduce statistical error bars,
- 10^6 incident particles towards the spacecraft shielding for each run.

Main parameters for the simulations of the lens coating contribution are given below:

- mono-energetic (4 MeV) alpha particles of normal incident direction with respect to the detector,
- 10 runs in order to reduce statistical error bars,
- 10^4 incident particles towards the detector for each run.

For one run of 10^6 incident particles, simulations were running during 9 min on a SUN platform (Enterprise 3000 using 1 processor at 450 MHz). This led to less than 40 hours of computation time for the simulation of GCRs (protons and alphas). Computation time for the lens coating contribution was negligible due to the relative simplicity of the geometrical model in this case.

Energy deposits have been recorded in a 3-dimensional space (x,y,E) representing respectively the pixel coordinates and the amount of deposited energy. Images of synthetic glitches have been produced (see Fig. 6). They are very similar to real data (compare with Fig. 3). We have also derived the length and the individual energy deposit for each track. It was thus easy to compute statistics on simulated glitches.

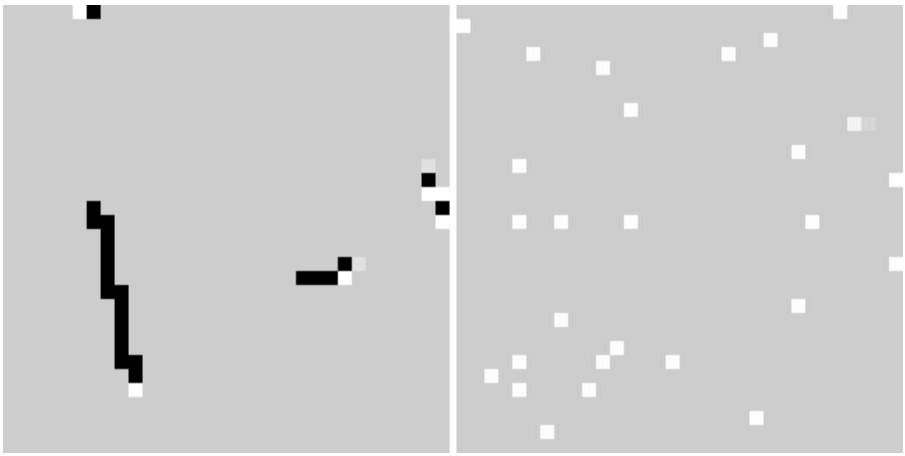

Figure 6. Images of synthetic glitches produced with the GEANT code. Left panel represents the contribution of galactic protons with an average energy of 600 MeV for a 5 s integrated LW image. Right panel represents the contribution of alpha particles produced by the radioactive lens coating (^{232}Th) for a 10 min integrated LW image.

Full distributions of interesting parameters (such as deposited energy, particle track length, glitch rate, ...) were then available.

Note that the GEANT code was used to simulate only the particle transport, not the radiation impacts on the electronics or the readout circuits. For example, it would have been very interesting to model the distribution of charge collection over time, but this was out of the scope of this paper. Nevertheless, such a model would be necessary in order to understand better the phenomenology of Type-C "dipper" glitches. For example, when the LET of incoming particle is very high, the internal electric field can be modified by the large amount of created charges, leading to negative current, typical of Type-C glitches. See Claret et al. (1999) for more details about this phenomenon.

5. Results

Because of the low sensitivity to particle impacts of the SW detector (see Section 3.1 and 3.2), only LW glitches are addressed here.

5.1. Galactic Protons

The particle track length and energy deposit produced by galactic protons have been computed as a function of the energy of incident particles (see Fig. 7). The average length of track is 8 pixels/glitch. This computed value is in very good agreement with the expected value for galactic particles (see Section 3.2). The increase of track length visible in Fig. 7 towards low energy is due to the detector geometry. Below 80 MeV/n the aluminum shell stops particles. Between 80 MeV and 120 MeV they can traverse the aluminum shell but are stopped by the titanium slabs, so that only the particles with a grazing incidence (i.e. passing between the titanium slabs) can traverse the detector. Such a particle traverses the detector in the horizontal plane, leading to track length in the range of 20-30 pixels. The energy deposition increase, also visible in Fig. 7 towards low energy, is due to both geometrical effect and ionizing power, which increases when the particle energy decreases.

Distribution of deposited energy by galactic protons is displayed on Fig. 8. The average deposited energy is around 600 KeV, which is compatible with expected values (Ziegler et al., 1985; Ziegler et al., 1977).

Contribution of galactic protons to the glitch rate as a function of the energy of incident particle has been computed (see Fig. 9). The total glitch rate from galactic protons is 0.83 ± 0.12 glitch/s. This value takes into account both the number of direct impacts which represent 0.36 glitch/s, and the number of secondary impacts.

5.2. Galactic Alphas

The particle track length and energy deposit produced by galactic alphas have been computed as a function of the energy of incident particle (see Fig. 10). Due to the isotropic origin of galactic alphas, the average length of track is also around 8 pixels (see Section 3.1). The average energy deposit by alpha particles is around 2.4 MeV, as computed by simulations, is also compatible with expected values (Ziegler et al., 1985; Ziegler et al., 1977). In spite of having a larger stopping power than protons, galactic alpha particles do not stop in the detector because of their high incident energy. Contribution of galactic alphas to the glitch rate as a function of the energy of incident particle has been computed (see Fig. 11). The total glitch rate from galactic alphas is 0.045 ± 0.026 glitch/s.

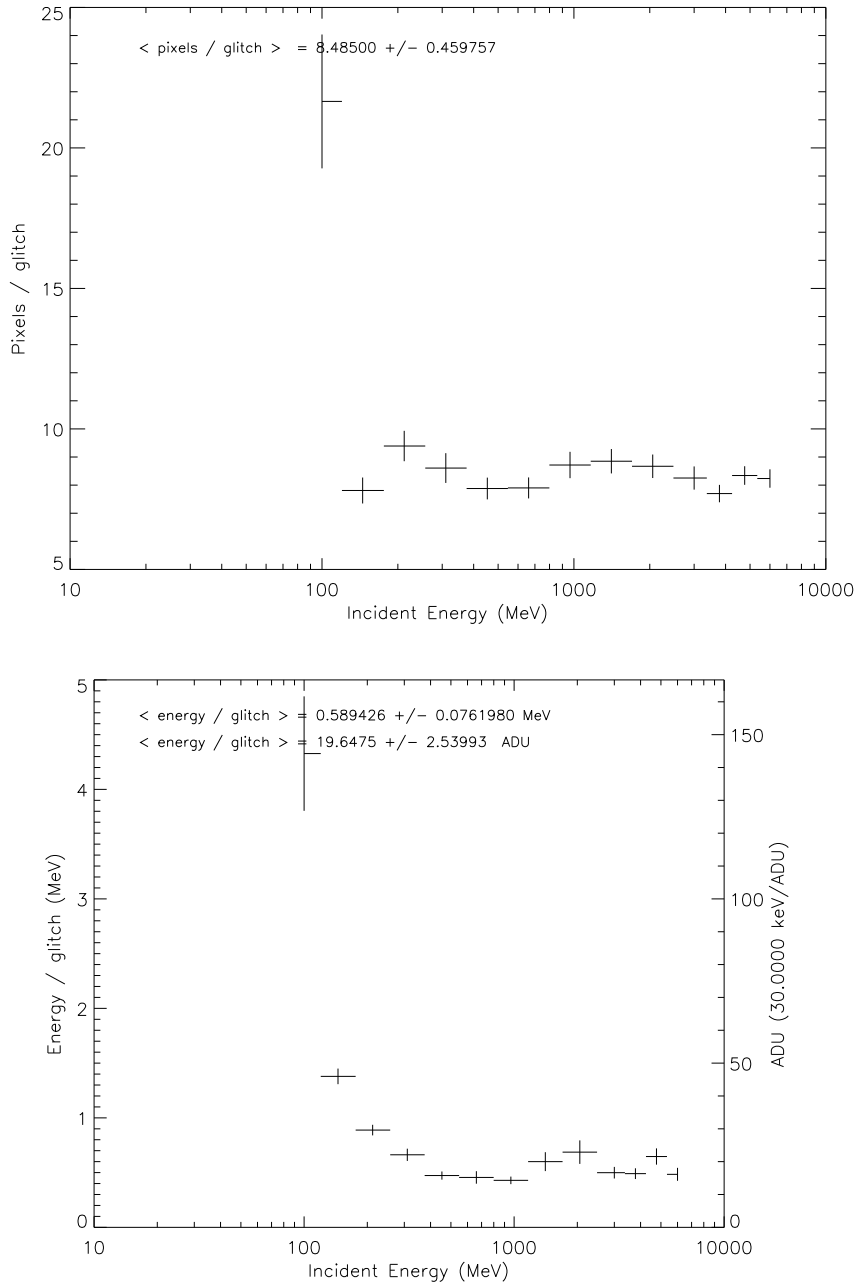

Figure 7. Spatial and temporal properties of glitches produced by galactic protons as a function of the energy of incident particle, computed by Monte-Carlo simulations. The mean number of pixels per glitch is 8.5 ± 0.5. The mean energy per glitch is 590 ± 80 KeV.

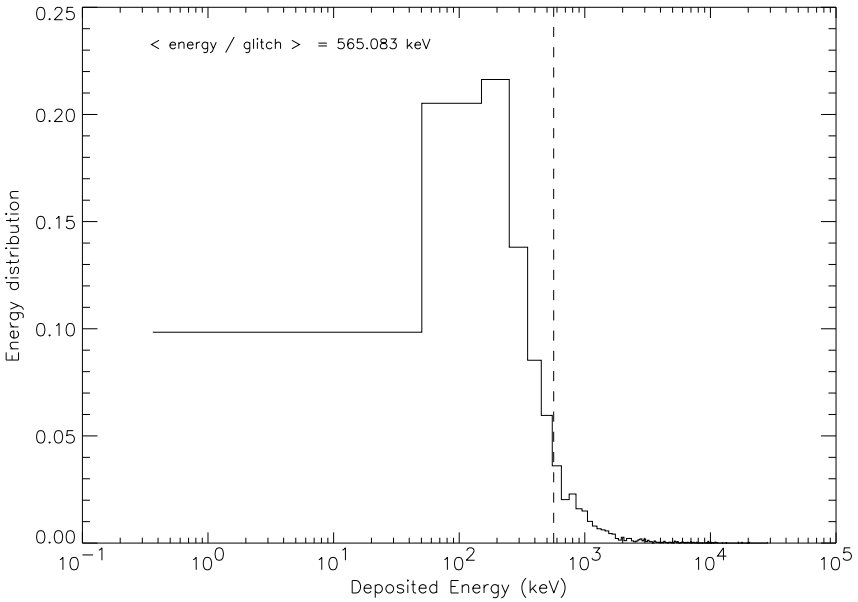

Figure 8. Distribution of deposited energy by galactic protons as computed by Monte-Carlo simulations.

5.3. Alphas from Lens Anti-Reflecting Coating

This contribution of alpha particles from the anti-reflecting coating was also simulated. Due to the quasi-normal incidence of these particles and their low energy, they induce small glitches of only one or two pixel length, increasing the overall detector noise (see Fig. 6). Nevertheless, if we consider a 5 sec integrated image and the most used lens (6 arcsec/pixel), we get less than 1 glitch/sec.

6. Discussion

6.1. Comparison With Predictions

Monte-Carlo results are summarized in Table II. The computed value for the average glitch length is in very good agreement with the expected value. This is quite obvious if we keep in mind that we assumed an isotropic shielding and an isotropic distribution for galactic incoming particles (see Section 3.1). But in the case of a less isotropic shielding distribution, these kind of simulations are very useful to determine glitch characteristics.

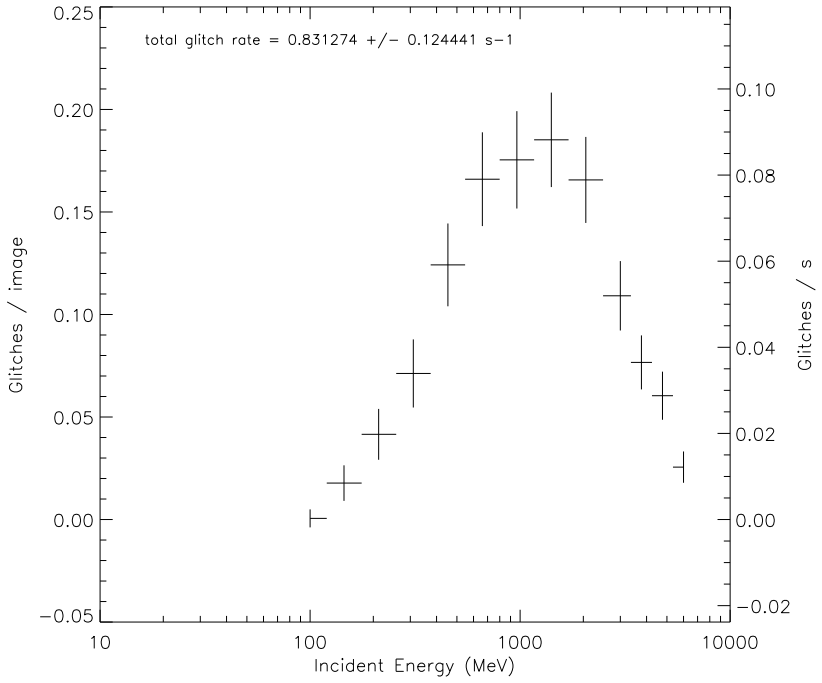

Figure 9. Contribution of galactic protons to the glitch rate as a function of the energy of incident particle, computed by Monte-Carlo simulations. The total glitch rate from galactic proton is 0.83 ± 0.12 s^{-1}.

Considering the above computed values for the total glitch rate from galactic particles (0.83 s^{-1} for protons and 0.045 s^{-1} for alphas), plus the contribution of alpha particles from ^{232}Th, we get a total glitch rate of 1 glitch/s. This computed value is in very good agreement with the expected glitch rate (see Section 3.2.). The total glitch rate for galactic particles is 0.87 s^{-1}. Considering that there is 0.36 s^{-1} for direct impacts, this leads to 0.51 s^{-1} for secondary impacts. The contribution of secondary particles and δ-rays represents about 60% of the direct impacts.

It would be interesting to compare the distributions generated by Monte-Carlo simulations with those derived directly from in-flight data. Unfortunately, a strong difficulty comes from the necessity of detecting glitches individually in the data. An advanced pattern recognition algorithm would be necessary to extract individually all glitches from the data, and then build their statistics. On the contrary, Monte-Carlo simulation can be of great help in order to predict these distributions, and use them for optimization purposes. For example, this can have a major

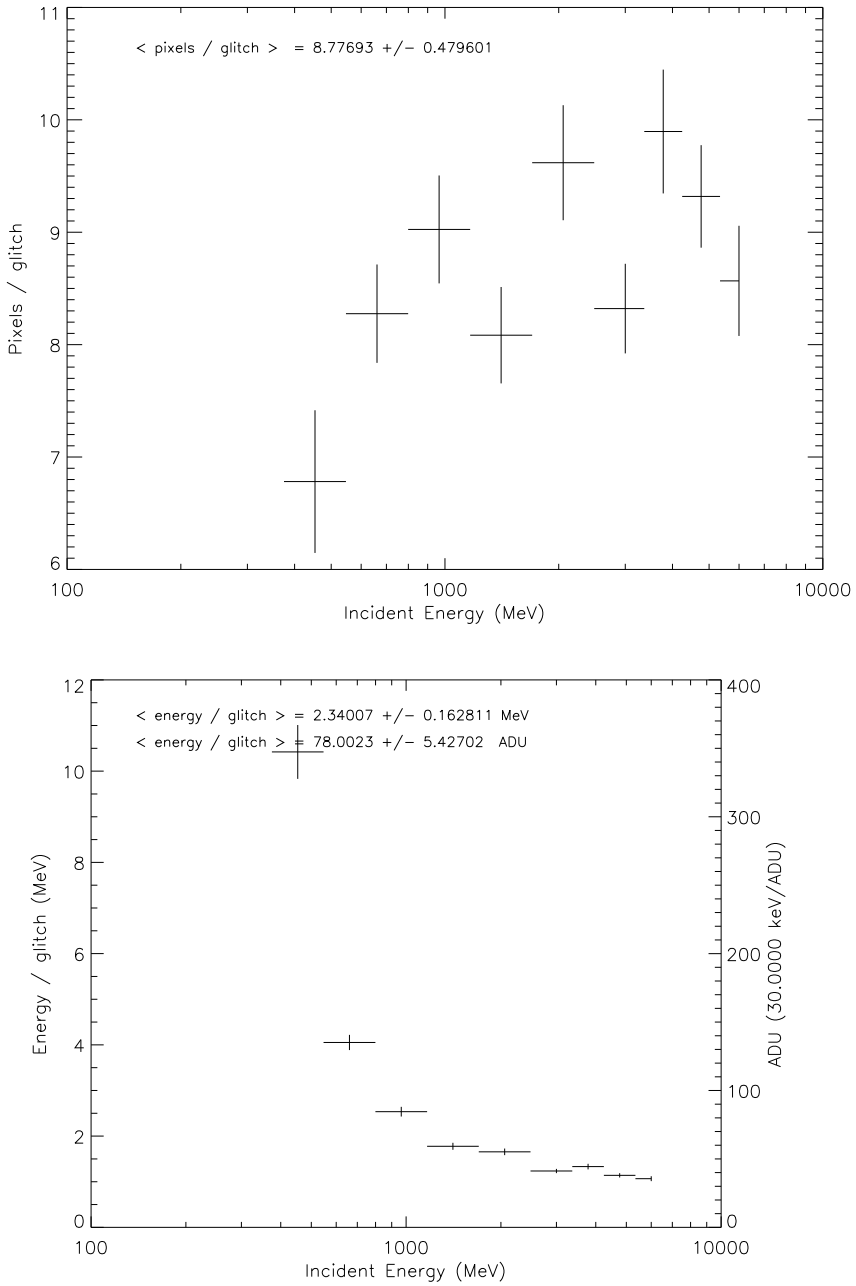

Figure 10. Spatial and temporal properties of glitches produced by galactic alphas as a function of the energy of incident particle, computed by Monte-Carlo simulations. The mean number of pixels per glitch is 8.8 ± 0.5. The mean energy per glitch is 2340 ± 163 KeV.

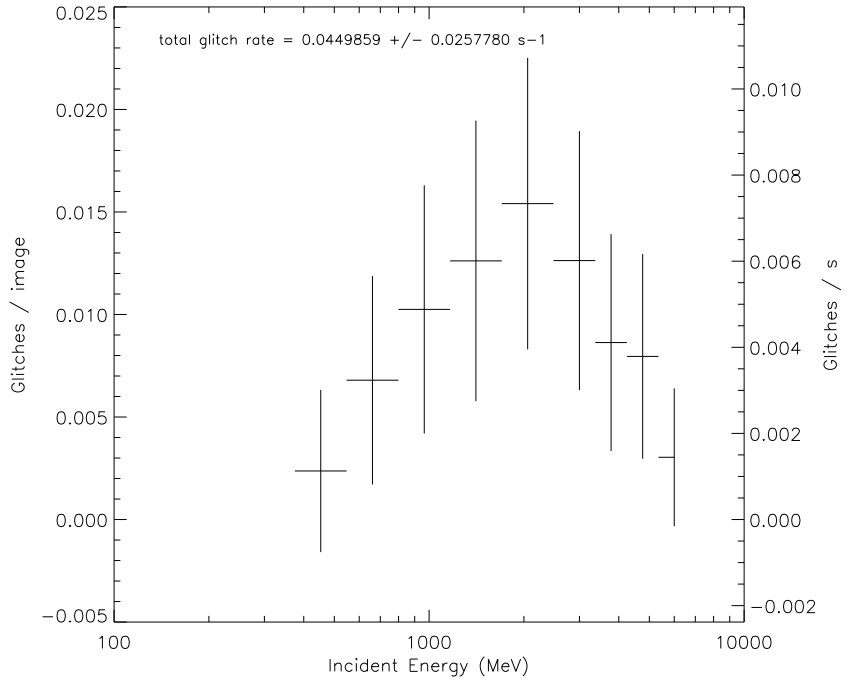

Figure 11. Contribution of galactic alphas to the glitch rate as a function of the energy of incident particle, computed by Monte-Carlo simulations. The total glitch rate from galactic alphas is 0.05 ± 0.025 s^{-1}.

influence in the choice of materials in the immediate surroundings of the detector.

Table II. Summary of Monte-Carlo results (Energies are in MeV, lengths in pixel units and glitch rates in s^{-1}). Values marked with the asterisk depend on the lens in use. Total rate should be understood as the primary + secondary contributions of a particle.

	Protons of GCRs	Alphas of GCRs	alpha particles from lenses
Typical incident energy	600	2000	4
Deposited energy	0.59±0.08	2.34±0.16	4
Track length	8.5±0.5	8.8±0.5	1-2*
Total rate	0.83±0.12	0.045±0.026	0.002-0.35*

6.2. Applications

There are several kinds of applications derived from Monte-Carlo simulations. It is very convenient to have, before launch, a clear idea of sensitivity loss induced by particle impacts. For example, several integration times were available for LW images (0.28, 2.1, 5.04, 10.08 and 20.16 s). But for 20 s images, it appeared that it was very difficult to deglitch data due to the high number of glitches per image (around 20 glitches of 8 pixels each). For this reason, ISOCAM operators were advised to avoid using 20 s integration time. This could have lead to strong consequences on the feasibility of some specific scientific programs. Monte-Carlo simulations performed before launch would have allowed to anticipate this situation. More generally, simulated images of realistic particle effects allow to test various algorithms of glitch removal before the launch of the space experiment. It is easy to add some noise to simulated images in order to test the actual efficiency of algorithms. If one can be satisfied with the efficiency of removal algorithm on ground, on board removal can then be envisaged, rather than down-linking raw data and perform glitch removal on the ground. This can help to solve the problem of prohibitive huge data volume to be down-linked to the ground station.

Our simulation tool has been compared with real data from the ISO spacecraft. It will be used for the prediction of radiation effects on HERSCHEL/PACS (Photo-conductor Array Camera and Spectrometer) bolometer detectors. Their very low operating temperature (300 mK) implies a very low heat capacitance so that the cosmic rays will induce local warm-up of the detectors when they pass through it.

7. Conclusions

The sensitivity of the ISOCAM is limited by glitches caused by impacts of charged particles. Outside the trapped radiation belts the observed glitch rate is about 1 glitch/s. The direct impact of GCRs represents about one third of this figure. The remainder comes from secondary particles, mainly nuclear interaction particles and δ-rays. Glitch rates, as well as spatial and energetic properties of glitches, have been computed by Monte-Carlo simulations. They are in good agreement with both the measured and expected values. This simulation tool can be used in order to predict the effect of incoming particles on future space experiments.

Acknowledgements

The authors would like to acknowledge Philippe Laurent for his help on the GEANT code.

References

CERN Geneva, Switzerland, *GEANT - Detector Description and Simulation Tool, CERN Program Library Long Writeup W5013*, http://cern.ch/cernlib

C. Cesarsky, A. Abergel, P. Agnèse, et al., *ISOCAM in flight*, Astronomy and Astrophysics, 315, L32, 1996.

A. Claret, H. Dzitko, J.J. Engelmann and J.-L. Starck, *Glitch effects in ISOCAM detectors*, Experimental Astronomy, vol. 10, Nos 2-3, pp. 305-318, 2000.

A. Claret, H. Dzitko and J.J. Engelmann, *Transient particle effects on the ISOCAM instrument on-board the Infrared Space Observatory*, IEEE Trans. on Nucl. Sci., vol. 46, no. 6, pp. 1511-1518, Dec 1999.

H. Dzitko, A. Claret and J.J. Engelmann, *Cosmic ray effects on the ISOCAM long wave detector*, Experimental Astronomy, vol. 10, Nos 2-3, pp. 279-290, 2000.

B. Heber and P. Ferrando, *CEA-SAP*, private communication.

M.F. Kessler, J.A. Steinz, M.E. Anderegg, et al., *The infrared space observatory (ISO) mission*, Astronomy and Astrophysics, 315, L27, 1996.

J.R. Letaw, *Space Radiation*, A commercial code available from Space Radiation Associates.

C. Paizis, A. Raviart, B. Heber, et al., *Rigidity dependence and time response of cosmic rays to the modulation steps in the rising part of solar cycle 23. COSPIN/KET results*, Space Sci. Rev., 97, 349-354, 2001.

J.A. Simpson, J.D. Anglin, A. Balogh, et al., *The Ulysses cosmic-ray and solar particle investigation*, Astronomy and Astrophysics Suppl., 92, 365-399, 1992.

J.D. Sullivan, *Geometrical factor and directional response of single and multi-element particle telescopes*, Nuclear Instruments and methods, 95, 5-11, 1971.

J.F. Ziegler, J.P. Biersack and U. Littmark, *The stopping power and range of ions in solids*, Pergamon Press, Oxford, 1985.

J.F. Ziegler, J.P. Biersack and U. Littmark, *Hydrogen stopping powers and ranges in all elements Stopping and ranges of ions in matter*, Pergamon Press, New-York, 1977.